

AD-A269 934



FASTC-ID(RS)T-0222-93

2

# FOREIGN AEROSPACE SCIENCE AND TECHNOLOGY CENTER



CARBON/CARBON COMPOSITES COATED WITH SiC BY CHEMICAL VAPOR DEPOSITION

by

Sun Shoujin, Liu Wenchuan, Li Minjun



DTIC  
ELECTE  
SEP 29 1993  
S E D

Approved for public release;  
Distribution unlimited.



93-22449



**HUMAN TRANSLATION**

FASTC-ID(RS)T-0222-93      14 September 1993

MICROFICHE NR: 93000552

CARBON/CARBON COMPOSITES COATED WITH SiC  
BY CHEMICAL VAPOR DEPOSITION

By: Sun Shoujin, Liu Wenchuan, Li Minjun

English pages: 16

Source: Cai Liao Gong Cheng, Nr. 4, August 1992;  
pp. 1-4

Country of origin: China

Translated by: Leo Kanner Associates  
F33657-88-D-2188

Requester: FASTC/TATV/Ernest S. Muller

Approved for public release; Distribution unlimited.

<p>THIS TRANSLATION IS A RENDITION OF THE ORIGINAL FOREIGN TEXT WITHOUT ANY ANALYTICAL OR EDITORIAL COMMENT STATEMENTS OR THEORIES ADVOCATED OR IMPLIED ARE THOSE OF THE SOURCE AND DO NOT NECESSARILY REFLECT THE POSITION OR OPINION OF THE FOREIGN AEROSPACE SCIENCE AND TECHNOLOGY CENTER.</p>	<p>PREPARED BY:  TRANSLATION DIVISION FOREIGN AEROSPACE SCIENCE AND TECHNOLOGY CENTER WPAFB, OHIO</p>
--	---

GRAPHICS DISCLAIMER

All figures, graphics, tables, equations, etc. merged into this translation were extracted from the best quality copy available.

Accession For	
NTIS CRA&I	<input checked="" type="checkbox"/>
DTIC TAB	<input type="checkbox"/>
Unannounced	<input type="checkbox"/>
Justification .....	
By .....	
Distribution/	
Availability Codes	
Dist	Avail and/or Special
A-1	

CARBON/CARBON COMPOSITES COATED WITH SiC  
BY CHEMICAL VAPOR DEPOSITION

Sun Shoujin, Liu Wenchuan, and Li Minjun

Institute of Metallography, Chinese Academy of Sciences

[Abstract] Oxidation-resistant carbon/carbon (C/C) composites were fabricated by chemical vapor deposition (CVD) of SiC on the surface of C/C composites; the latter were densified in preforms of carbon cloth lay-up by chemical vapor infiltration (CVI) of carbon. The mechanical properties, thermal properties, and the oxidation resistant properties in air of the material are studied.

## I. Introduction

Because of excellent high-temperature mechanical properties and thermophysical properties, C/C composites have wide applications. Like conventional carbon material, C/C composites will have obvious oxidation in oxidizing environments at temperatures higher than 500<sup>o</sup>C [1].

Numerous studies were made of the oxidation resistant problem of C/C composites by impregnating the surface with inorganic salts (such as B<sub>2</sub>O<sub>3</sub> and ZnPO<sub>4</sub>, etc.), and borate-based

ply [2] containing refractory particles, as well as coating the surface with BN and TiC plies [3,4], or filling the substrate carbon with  $B_2O_3$  [5] to the extent that the material can resist oxidation only at intermediate temperatures (lower than  $1200^{\circ}C$ ). For high-temperature oxidation resistance (at temperatures higher than  $1300^{\circ}C$ ), generally SiC and  $Si_3N_4$  coating plies are used. Conventionally, the solid infiltration method and the CVD method [6] are employed to form an SiC coating ply on the C/C composite surfaces.

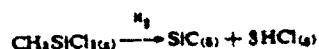
The paper describes the CVD method for surface deposition of an SiC ply with carbon cloth lay-up of 2D-C/C composite surface along with the technical parameters, structure, and properties.

## II. Experimental Section

### 1. Preparation of materials

Lay up the PAN carbon fiber cloth, which was made at the Jilin Carbon Plant, after cutting to specifications; there are six carbon cloth plies per each millimeter of thickness. Nitrogen is used as the diluent gas, and acetylene is used as the starting material gas; after carbonization with the CVD method so that its density is  $1.6g/cm^3$ , then methyl silicon trichloride ( $CH_3SiCl_3$ ) is used as the starting material, while hydrogen and argon are, respectively, the carrier gas and the diluent gas. SiC is deposited on the surface of the densified C/C material. To prevent the appearance of free silicon or free carbon in the deposit, the compounding ratio between hydrogen and  $CH_3SiCl_3$

(which are admitted to the deposition chamber) should be appropriately selected. The general formula for dissolving  $\text{CH}_3\text{SiCl}_3$  is as follows:



Refer to Table 1 for technical parameters during material preparation.

TABLE 1. Preparation of C/C Composites and SiC Deposition Ply

沉积材料 1	沉积温度 (°C) 2	炉压 (Pa) 3	原料气体流量 (m³/h) 4		稀释气体流量 (m³/h) 5		最终材料 密度 (g/cm³) 6
			C₂H₂	CH₃SiCl₃ + Ar	N₂	H₂	
C	1100	1000	0.02		0.07		1.6
SiC	1250	1000		0.02		0.06	

KEY: 1 - Deposition ply    2 - Deposition temperature  
 3 - Furnace pressure    4 - Flow rate of starting material gas  
 5 - Flow rate of diluent gas    6 - Density of final material

## 2. Measurement and testing of properties

The measurement and testing of the mechanical properties are conducted on a universal electronic tester. The loading rate is 0.5mm/min. The direction of elongation is parallel to the surface of the carbon cloth ply. Compression, bending, and shearing are loaded in two directions: parallel and perpendicular to the surface of the carbon cloth ply.

The coefficient of thermal expansion is measured on a quartz thermal expansion instrument, from room temperature to 900°C.

The test direction is parallel to the surface of the carbon cloth ply.

Thermal conductivity is tested on a laser thermal conductivity instrument by using specimens OD 10mm x 2mm; the heat flow is perpendicular to the cloth surface.

Oxidation resistance of the material is tested on a muffle furnace and a microthermal balance; the oxidation temperature is 1300°C and the oxidation period is 1h.

### III. Experimental Results and Discussion

#### 1. Structure of material

Refer to Figs. 1 and 2 for the metallographic structure of the material. During the gas-phase carbonization process, pores in the fiber bundle and between fiber bundles are filled and closed by thermally disintegrated carbon. On the metal surface, silicon carbide forms a homogeneous and continuous deposition ply on the material surface. The ply thickness is approximately 20micrometers.



Fig. 1. Internal structure of oxidation-resistance C/C material. x75



Fig. 2. SiC surface deposition ply on oxidation-resistance C/C composites. x200

As indicated by X-ray diffraction analysis of the material, under the conditions of this process the deposited materials are SiC and beta-SiC (Fig. 3).

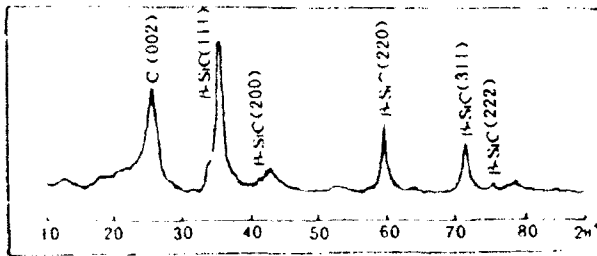


Fig. 3. X-ray diffraction spectrum of SiC (Cu  $k_{\alpha}$ )

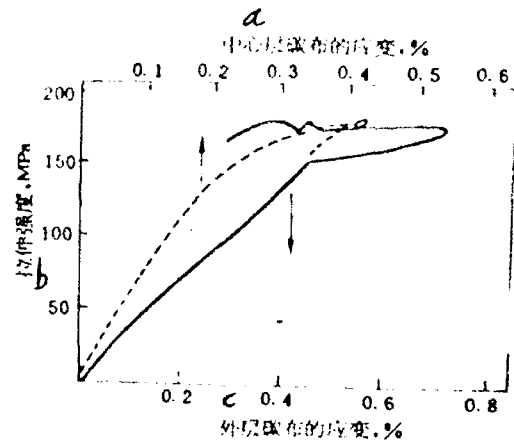


Fig. 4. Elongation stress-strain curve of oxidation-resistance C/C material

KEY: a - Strain of center ply carbon cloth b - Elongation strength c - Strain of outer ply carbon cloth

## 2. Mechanical and thermophysical properties of oxidation-resistant C/C materials

Table 2 shows the elongation properties and elongation strain of composite materials, as collected from strain sheets cemented on the outer-ply carbon cloth and the central ply carbon cloth. From these results, the strain in the outer-ply carbon cloth materials is 60 percent higher than the strain in the central-region carbon cloth. From this fact, the stress-strain distributions at the specimen cross-section are not uniform. The stress at the outer-ply carbon cloth is higher than in the inner ply carbon cloth. At the stress level lower than the elongation strength of the material, the strain in the outer-ply carbon cloth is stagnant and even decreasing (refer to Fig. 4). This indicates that before breakdown of the entire specimen, the outer-ply carbon cloth has been ruptured. The elongation and the rupture process of composite materials proceed first from the outer-ply carbon cloth, and gradually spreads to the inner-ply carbon cloth. The cause of this phenomenon is that the binding strength between carbon cloth plies for composite materials is relatively low and is not sufficient to transmit the loading of the outer-ply carbon cloth toward the inner-ply carbon cloth; therefore, mainly the stress concentrates in the outer-ply carbon cloth.

The process of compressive rupture differs along the directions perpendicular to and parallel to the carbon cloth

surface plies (Fig. 5). The compressive strength and the rupture strain along the direction parallel to the cloth surface are much lower than that along the direction perpendicular to the cloth surface (refer to Table 3). When loading in the direction parallel to the cloth surface, the compressive rupture change of the material is exhibited as spreading along the direction of the cloth surface, finally causing the material to rupture along the cloth surface. However, for loading perpendicular to the cloth surface, the material appears to have very high pseudoplasticity. The initial linear elastic region is mainly due to the function of the SiC deposition ply. At this stage, the modulus approaches the modulus of elasticity of beta-SiC. After the SiC deposition ply ruptures, the material appears to exhibit pseudoplastic behavior. At this stage, inner pores of the material are compressed and disappear, thus the material is compacted. Finally, the material ruptures.

TABLE 2. Elongation Properties of Materials

性能 a		平均值 b	测试结果范围 c	试样个数 d
拉伸强度 (MPa) e		221	185~245	5
弹性模量 f (GPa)	布面 h	41.3	35.0~39.4	5
	层面中心 i	63.0	51.5~74.9	3
断裂应变 g (%)	布面 h	0.66	0.45~0.79	5
	层面中心 i	0.41	0.36~0.44	3

\* This value is the stress at initial rupture  
 KEY: a - Properties    b - Mean value    c - Range of test results    d - Number of specimens  
 e - Elongation strength    f - Modulus of elasticity    g - Rupture strain\*    h - Cloth surface  
 i - Center of ply surface

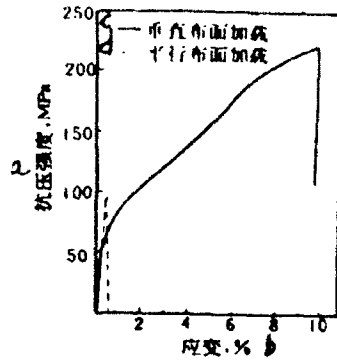


Fig. 5. Compressive stress-strain plot of the material  
 KEY: a - Compressive strength b - Strain  
 c - Loading in direction perpendicular to cloth surface d - Loading in direction parallel to cloth surface

TABLE 3. Compressive Rupture Properties of Material

性能 a		平均值 b	测试结果范围 c	试样个数 d
e 平行布面	压缩强度 (MPa) g	90.9	63.2~136	8
	弹性模量 (GPa) h	48.8	26.7~86.3	8
	破坏应变 (%) i	0.222	0.141~0.323	8
f 垂直布面	压缩强度 (MPa) g	217	200~239	8
	弹性模量 (GPa) h	1.79	1.53~2.09	3
	破坏应变 (%) i	9.54	9.36~9.65	3

KEY: a - Properties b - Mean value c - Range of test results d - Number of test specimens  
 e - Parallel to cloth surface f - Perpendicular to cloth surface g - Compressive strength  
 h - Modulus of elasticity i - Rupture stress

When loading along a material in a direction parallel to, and in a direction perpendicular to the cloth surface, the bending properties of the material differ. The bending strength and the rupture strain along the direction perpendicular to the cloth surface are higher than in the direction parallel to the

cloth surface (refer to Table 4). However, when loading along both directions, the process of bending and rupture exhibits a basically similar trend (refer to Fig. 6). When loading along the direction perpendicular to the cloth surface, the strain in different ply surface differs; carbon cloth in the upper half is under compressive stress, but carbon cloth in the lower half is under tensile stress; therefore, a shearing stress is induced between the carbon cloth plies. Under the action of inter-ply shearing stress, rupture occurs between carbon cloth plies. When loading along the direction parallel to the cloth surface, in the process of bending rupture, the carbon cloth is bent, thus causing inter-ply rupture of the carbon cloth.

TABLE 4. Bending Properties of the Material

性能 a		平均值 b	测试结果范围 c	试样个数 d
e 平行 布面	弯曲强度 (MPa) g	60.0	50.6~74.9	6
	弹性模量 (GPa) h	41.0	20.7~41.9	6
	断裂应变 (%) i	0.398	0.265~0.538	6
f 垂直 布面	弯曲强度 (MPa) g	193.0	141.9~271.4	5
	弹性模量 (GPa) h	34.0	32.8~34.7	3
	断裂应变 (%) i	0.811	0.564~1.520	5

KEY: a - Properties    b - Mean value    c - Range of test results    d - Number of test specimens  
 e - Parallel to cloth surface    f - Perpendicular to cloth surface    g - Compressive strength  
 h - Modulus of elasticity    i - Rupture stress

As further indicated by the shearing rupture experiments performed on the material, the shearing strength along the direction perpendicular to the cloth surface is much lower than

that parallel to the cloth surface (refer to Table 5). The weakest sector of the material is the inter-ply strength of the carbon cloth.

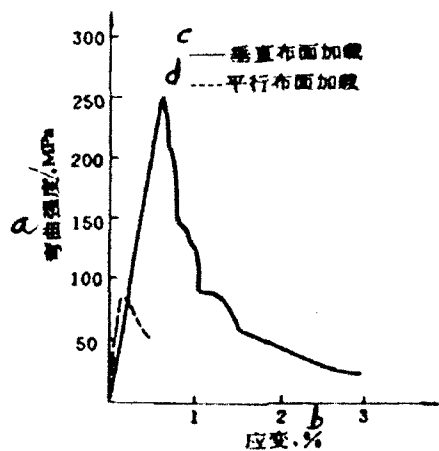


Fig. 6. Bending stress-strain plots of oxidation-resistant C/C material  
 KEY: a - Bending strength    b - Strain  
 c - Loading along direction perpendicular to cloth surface    d - Loading along direction parallel to cloth surface

TABLE 5. Shearing Strength of the Material

性/能 a	平均值 b	测试结果范围 c	样品数 d
层间剪切强度 (MPa) e	9.71	8.35~12.0	8
断纹剪切强度 (MPa) f	58.7	52.8~71.5	7

KEY: a - Properties    b - Mean value    c - Range of test results    d - Number of specimens  
 e - Inter-ply shear strength    f - Rupture shear strength

Figs. 7 and 8 show, respectively the variation plots versus temperature for the thermal expansion coefficient and thermal conductivity of oxidation-resistant C/C material. As found in experiments, the variation with temperature is reversible for the

thermal expansion coefficient of the material. After the specimen is cooled to room temperature, there is no residual thermal expansion. This indicates that basically, there is no residual thermal stress in the material. With a rise in temperature, the trend of increase in thermal conductivity becomes weaker and weaker. After the temperature attains 800°C, basically thermal conductivity does not rise further, at 6.58 W/m.K.

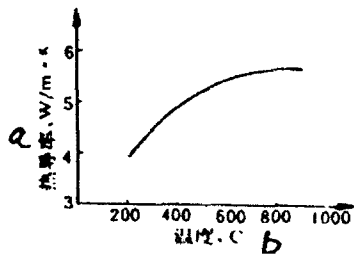


Fig. 7. Variation of thermal expansion coefficient [sic] versus temperature  
KEY: a - Thermal conductivity [sic] b - Temperature

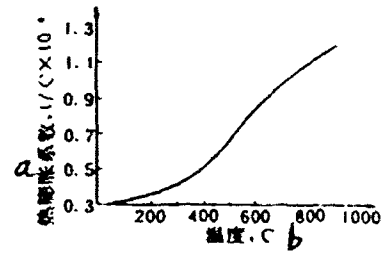
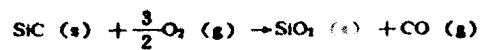


Fig. 8. Variation of thermal conductivity [sic] versus temperature  
KEY: a - Thermal expansion coefficient [sic] b - Temperature

### 3. Oxidation-resistant properties of the material

The main shortcoming of C/C composite materials is their sensitivity to air oxidation at high temperatures. Deposited on the surface of C/C material, the SiC deposition layer forms a layer of thin, but stable glassy-state SiO<sub>3</sub> film at a high temperature upon reaction with oxygen:



The film has higher capability in resisting air oxidation, thus effectively protecting the C/C material.

However, since there are major differences in thermal expansion coefficients between C/C material and SiC deposition layer, after the material is heated and then cooled, obvious cracks are generated in the surface of the coating layer (see Fig. 9); these cracks are channels for expansion of oxygen from inside the specimen. Fig. 10 shows the relationship curves of weight loss due to oxidation and the oxidation weight loss rate versus time for the material at 1300°C. We can see that with prolonged air oxidation time period, the oxidation weight loss of the material gradually increases; however, the rate of increase gradually declines; that is, the rate of weight loss due to oxidation maintains a trend of moderate reduction.

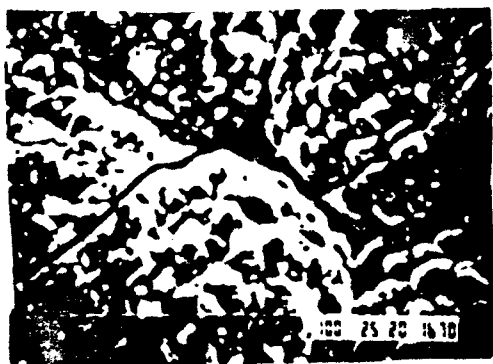


Fig. 9. Cracks in SiC coating layer on surface of material

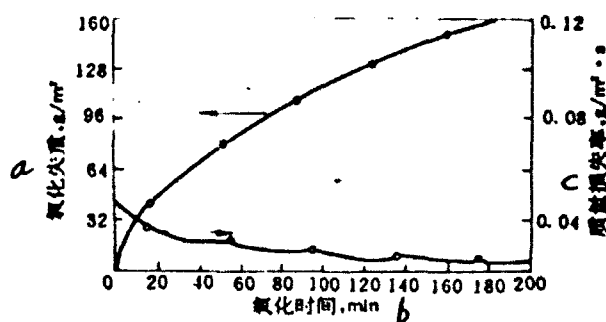


Fig. 10. Variation plots of weight loss due to oxidation, and rate of weight loss due to oxidation versus time  
 KEY: a - Weight loss due to oxidation b - Oxidation time period c - Rate of mass loss

Oxidation of C/C composite materials with an SiC deposition layer is caused by the following process: when air passes through the SiC deposition layer, its defects diffuse toward the layer interior, thus oxidizing the C/C material at the bottom of the SiC deposition layer. The oxidation process includes two steps: the chemical reaction between carbon and oxygen, and the gas-phase diffusion process prior to the reaction; the diffusion process includes the entrance of oxygen into the material and the vaporization of CO and CO<sub>2</sub>, the reaction products. Under different conditions, there are different processes controlling the oxidation rate. In the view of Yusuda et al. [7], at lower temperatures, the oxidation process is mainly controlled by the oxidation reaction; however, at higher temperatures, the oxidation process is controlled by gas-phase diffusion. There are different temperatures at the boundary point for different material structures, and materials after different treatments.

According to the results of oxidation experiments on the microthermal balance, the weight loss and the logarithm of the weight loss rate due to oxidation of oxidation-resistant C/C material satisfies a linear relationship (refer to Fig. 11); this indicates that the oxidation process at 1300°C for C/C composite material coated with an SiC deposition layer is controlled by means of gas-phase diffusion prior to reaction.

To compensate for the influence of oxidation-resistant properties on material due to defects in the deposition layer, a B<sub>2</sub>O<sub>3</sub> impregnated specimen is employed so that B<sub>2</sub>O<sub>3</sub> can fill up

nfilt  
hat t  
he bi  
ateri

the cracks in the deposition layer. For the post-impregnated material, after 1h oxidation in air at 1300°C, the mass loss rate is 0.036g/m<sup>2</sup>.s; the rate is much lower than the oxidation rate of material without impregnation.

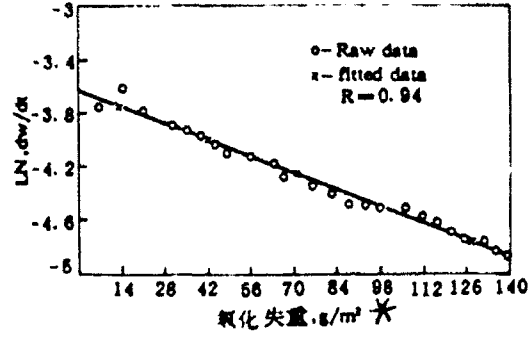


Fig. 11. Relationship between oxidation weight loss and logarithm of oxidation weight loss rate  
KEY: \* - Oxidation weight loss

onclus  
1.  
arbon  
idati  
ay-up  
nding

With instantaneous heating and cooling, and purging with a hot air stream, a complete or incomplete deposition layer is an effective way of evaluating the binding strength between the deposition layer and the substrate. Therefore, with thermal insulation by means of a quartz lamp on the material, purging with a hot exhaust gas stream from the engine and hot vacuum experiments are conducted on the material; the experimental results are listed in Table 6. After purging with an exhaust gas stream from the engine and thermal insulation with a quartz lamp, there are different degrees of cracks and droppings for the SiC deposition layer. This indicates that the binding between the SiC deposition layer and the C/C material should be strengthened. In particular, based on the properties of the chemical gas-phase

infiltration, SiC is deposited deep in the opening gas pores so that the SiC is rooted inside the C/C material, thus upgrading the binding strength between the deposition layer and the material.

TABLE 6. Experimental Results of the Unique Properties of the Material

试验 a	条件 b	试验结果 c
石英灯隔热 试验 d	热流 502.41kW/m <sup>2</sup> 空气中 330s g	表面出现裂纹 h 背面温度 980°C
热真空 试验 e	真空度 4.0×10 <sup>-3</sup> MPa 1410°C 10min i	试样未出现表面裂 纹, 完好 j
发动机热 流冲刷试验 f	马赫数 0.4 K 气流温度 1455°C 时间 1min	试样表面涂层 l 出现开裂

KEY: a - Experiment b - Conditions c - Experimental results d - Thermal insulation experiment with quartz lamp e - Thermal vacuum experiment f - Experiment with purging with a hot exhaust stream from an engine g - Heat flow at 502.41kW/m<sup>2</sup> in air for 330s h - Cracks appearing at the surface; temperature at back surface is 980°C i - Degree of vacuum j - No surface cracks appeared in the specimen, which is desirable k - Mach 0.4; 1455°C in gas stream temperature; and 1min in time period l - Cracks appearing at the deposition layer on specimen surface

## Conclusions

1. In two directions, perpendicular and parallel to the carbon cloth surface, the mechanical properties are different for oxidation-resistance C/C composite material by using carbon cloth lay-up for reinforcement of its framework. The compressive, bending, and shearing strengths along the direction perpendicular

to the cloth surface are higher than the values parallel to the cloth surface.

2. Oxidation of C/C composite material protected by an SiC deposition layer is due to the following process: air diffuses from defects in the SiC deposition layer into the material interior to react with the carbon at the bottom of the SiC deposition layer. After impregnating with B<sub>2</sub>O<sub>3</sub>, the material has very high oxidation resistance at high temperatures.

3. After instantaneous heating, cooling, and purging with a powerful hot gas stream, the SiC deposition layer easily drops off. It is required to deposit SiC deep inside the C/C material in order to upgrade the binding force between the SiC deposition layer and the C/C substrate material.

## REFERENCES

1. Goto S. et al., Trans. ISJJ 26 (1986) 597
2. McKee D. W. Carbon, 4, 25 (1987) 551
3. Romainol J. Y. et al., Progress in Science and Engineering of Composites, Vol. 1 (1982) 1227
4. Hannae H. et al., J. Mater. Sci. 1, 19 (1984) 202
5. McKee D. W. Carbon, 5, 26 (1988) 659
6. Okamoto H. et al., Proc. 15th Int. Sym. on Space Tech. and Sci. Vol. 1 (1987) 529
7. Yuruda E. et al., Trans. JSCM 1, 6 (1987)

DISTRIBUTION LIST

DISTRIBUTION DIRECT TO RECIPIENT

<u>ORGANIZATION</u>	<u>MICROFICHE</u>
B085 DIA/RTS-2FI	1
C509 BALLOC509 BALLISTIC RES LAB	1
C510 R&T LABS/AVEADCOM	1
C513 ARRADCOM	1
C535 AVRADCOM/TSARCOM	1
C539 TRASANA	1
Q592 FSTC	4
Q619 MSIC REDSTONE	1
Q008 NTIC	1
Q043 AFMIC-IS	1
E051 HQ USAF/INET	1
E404 AEDC/DOF	1
E408 AFWL	1
E410 ASDTC/IN	1
E411 ASD/FTD/TTIA	1
E429 SD/IND	1
P005 DOE/ISA/DDI	1
P050 CIA/OCR/ADD/SD	2
1051 AFTT/LDE	1
PO90 NSA/CDB	1
2206 FSL	1

Microfiche Nbr: FTD93C000552  
FTD-ID(RS)T-0222-93